

An Extended Photometric Stereo Algorithm for Recovering Specular Object Shape and Its Reflectance Properties

Zuoyong Zheng¹, Lizhuang Ma¹, Zhong Li², and Zihua Chen^{3,4}

¹Department of Computer Science, Shanghai Jiaotong University, China
zuoyong.zheng@gmail.com, ma-lz@cs.sjtu.edu.cn

²Department of Applied Mathematics, Zhejiang Sci-Tech University, China
lizhongzju@hotmail.com

³Department of Computer Science, East China University of Sci-Tech, China

⁴State Key Laboratory for Novel Software Technology, Nanjing University, China
cjh@ecust.edu.cn

Abstract. In Photometric stereo, the existence of specularities hampers to recover the normal map. To deal with this common reflective phenomenon, we introduce a novel representation for specular reflection with a set of specular basis functions with different roughness values. This representation is suitable for any intensively or weakly specular object, and is introduced into the photometric stereo algorithm to recover both the surface shape and its reflectance properties. The reconstructed shapes and re-rendered images validate the proposed algorithm.

Keywords: Photometric Stereo, Specular Reflection, Surface Reconstruction.

1. Introduction

Photometric stereo is an important research field in computer vision, which is used to recover the shape of a static object under varying illuminations. Its first application was proposed by Woodham [1] in 1980's. The underlying principle is very simple: the normal at a surface point can be deduced from its intensity values caused by illuminations from different directions. The surface reflection is assumed to coincide with Lambertian diffuse model and the light source to be parallel. Obviously, pixel intensities are dependent on unknown surface orientations and known lighting directions. The photometric algorithm has three advantages: (1) no surface smoothness is assumed; (2) only multiple light sources are needed when implemented; (3) diffuse parameters can also be obtained. Due to these benefits, photometric stereo is widely used to reconstruct surface shape.

In traditional photometric stereo algorithms, ideal imaging conditions are generally assumed, i.e., Lambertian surface, distant light sources and orthographic camera projection. These constraints, especially the first, limit

the practical use of photometric stereo. The specularities exhibited by most real world objects violate the linear relationship between the pixel intensities and the normals, therefore make the solution deviate from the ground truth. The method coping with specular reflection can be classified into two categories. The first one is to identify and remove specularities using image-base techniques, while in the other group, specular pixels are directly used in analytic or discrete BRDF models. Due to the close coupling of surface shape and its reflectance properties, they are generally worked out simultaneously.

In this paper, an extended photometric stereo algorithm is proposed to recover the shape of a surfaces with specularities, and moreover, to recover its reflectance properties, thus falling into the second category dealing with specular reflection. The distinct feature of this method (also the main contribution of this paper) is to represent any possible specular reflection as a linear combination of a set of specular terms with preset roughness values. The actual specular reflection is projected onto such group of specular basis functions, and the resulting coefficients can be considered to represent the surface reflectance properties. Thus, all diffuse and specular pixels are utilized to recover both the shape and reflectance properties.

2. Previous Works

There are a lot of works to handle specular reflection in photometric stereo. Ikeuchi [2] first applied photometric stereo to specular surfaces. He used three extended light sources and then the reflectance maps for each source in the form of lookup tables. Nayar et al [3] used evenly distributed extended light source to identify accurately the diffuse and specular reflection, and used a so-called "photometric sampling" technique to calculate the surface orientation as well as the component of two kind of reflection. Kay and Caelli [4] used the simplified Torrance-Sparrow model [5] to describe reflectance properties, and introduced the simulated annealing algorithm into photometric stereo to simultaneously recover the normal map and the roughness parameter. Georgiades [6] used Torrance-Sparrow model to eliminate the ambiguity inherent in uncalibrated photometric stereo for diffuse objects. He established a complicated objective function incorporating all unknowns (reflection coefficients, surface normals, as well as light source intensities and positions). These unknowns are solved by an iterative non-linear optimization process. Shen et al [7] firstly recovered the specular reflectance parameters of the surfaces by a novel optimization procedure, then these parameters are used to estimate the diffuse reflectance and surface normal for each point. Chung and Jia [8] used the Ward model [9] to represent the reflectance properties, and calculated for shadow points their normals and BRDF parameters by using cast shadow information. These parameters are then taken into the Ward model for robustly estimating other points' normals and parameters using an iterative optimization.

Different from the aforementioned methods using analytic BRDF models, other works employed discrete, or data-driven models to replace non-linear BRDFs. Hertzmann and Seitz [10] proposed a smart and practical example-based solution to express reflectance properties, i.e., a purely diffuse ball and a snooker ball to respectively represent the diffuse and specular reflection. In order to calculate the normal at a surface point, all possible points on the two reference balls are searched to approximate its intensity using the linear combination of the two reference points' intensities in least square sense. It is essentially a finite search on reference spheres, and no requirement for geometric and radiometric calibration for the camera and the light sources is its merit.

Alldrin et al [11] firstly analyzed the property of isotropic BRDF models, then express it as a bivariate discrete function in a closed form. After assuming that object materials are made of several "fundamental" materials, they constituted an iterative scheme to simultaneously solve the discrete BRDF, the material weight map and surface normals. Comparing Hertzmann and Alldrin's works, we can find they are similar in spirit to each other, i.e., the idea of "finite fundamental materials" to represent any actual materials.

On the one hand, the existence of specularities makes shape recovery involved in time-consuming non-linear optimization; on the other hand, specularities strongly imply the symmetry between the light direction and view direction with respect to surface normals. Chen et al [12] proposed a photometric algorithm only using specularities. They firstly used the intensity histogram from multiple video frames to judge specular pixels, then computed the normals by using the calculated light position corresponding to that frame resulting in specular pixels. Because specularities are high frequency components in an image, a larger number of images are needed to judge their existence. To exceed this limitation, Francken et al [13] used a LCD monitor displaying binary black-white strip pattern as an array of light sources, instead of single point light source in Chen's work. Usage of such kind of coded light actually increases the light sampling rate, as a result, the required images are cut down.

In the remainder of this paper, we will describe and implement our extended photometric stereo algorithm, which belongs to the discrete-BRDF-model class. Our method is close in principle to Hertzmann's [10] and Alldrin's [11]. In comparison with the former, we used virtual reference objects (instead of actual ones), and express any specular reflection using a few fixed specular basis functions, therefore breaking the constraint that uses reference objects of nearly same specular appearance as the test objects. Compared to the latter, we estimate only surface normals and reflectance coefficients (incorporating their reflectance coefficients and material weight map), while ignoring the roughness estimation because fundamental materials is fixed in advance.

Our algorithm is outlined as follows:

- (1) Render images of virtual reference spheres corresponding to selected specular basis functions;

- (2) For each test object point, carry out a search on the reference spheres to approximate its intensity using reference sphere points' intensities in least square sense. The resulting normal and diffuse parameters are considered as accurate;
- (3) Cluster surface materials in terms of estimated diffuse parameters;
- (4) For each class of material, compute its specular coefficients according to an overdetermined linear equation system with inequation constraints while keeping each point's diffuse parameter fixed.
- (5) Render target objects' images under any illuminations and viewpoints.

The following assumptions are made: (1) isotropic reflection; (2) orthographic camera projection; (3) a single distant light source. The geometrical calibration of the light source (i.e., computing its directions) is needed, but the radiometric calibration (i.e., computing its absolute intensity) is not.

3. Principle

To express complex appearance of real world objects, Hertzmann and Seitz [10] suggest that all materials could be represent as a linear combination of a few fundamental materials. The mathematical expression is as follows:

$$I_p(L) = \sum_j \lambda_{j,p} f_j(\mathbf{n}_p, \mathbf{v}, L) \quad (1)$$

Here, I_p represents the point p 's pixel value, while its paramters L denotes the light directions. $f_j(\mathbf{n}_p, \mathbf{v}, L)$ is the reflectance model for the j th material (whose core is BRDF). Its parameter \mathbf{n}_p and \mathbf{v} are respectively the point p 's normal and the view direction. $\lambda_{j,p}$ represents the weight coefficient of the j th material. In the context of photometric stereo, L denotes different light directions, therefore I_p and f_j are all vectorial functions. If we see all f_j as independent basis functions, the pixel intensity is accordingly the consequence of their linear combination.

How to choose the basis functions $\{f_j\}$? We start from the Ward BRDF mode [9] which comprises a diffuse and a specular term:

$$BRDF_{Ward}(\mathbf{n}_p, \mathbf{v}, l) = BRDF_{Ward}(\theta_i, \theta_o, \sigma) = \frac{\rho_d}{\pi} + \frac{\rho_s}{\sqrt{\cos \theta_i \cos \theta_o}} \frac{\exp[-\tan^2 \sigma / \beta^2]}{4\pi\beta^2} \quad (2)$$

The parameters in Ward model are classified into two groups. The first group includes geometrical parameters θ_i , θ_o and σ , denoting respectively the angle between l (incident direction) and \mathbf{n}_p , \mathbf{v} and \mathbf{n}_p , as well as the angle between the halfway vector \mathbf{h} and \mathbf{n}_p (Fig. 1). The second group contains reflectance parameters ρ_d , ρ_s and β , representing respectively the diffuse and specular coefficient, as well as the roughness.

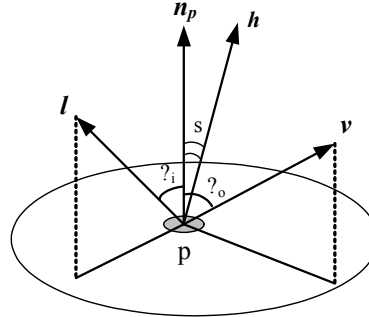


Fig. 1. Geometrical parameters in Ward BRDF

Taking into account the attenuation factor, the reflectance function f can be expressed as follows by means of the Ward model:

$$f(n_p, v, l) = f(\theta_i, \theta_o, \sigma) = \frac{L_0}{r^2} \cos \theta_i \text{BRDF}_{\text{Ward}}(\theta_i, \theta_o, \sigma) \quad (3)$$

Here, L_0 is the absolute light intensity, and r is the distance of target object from the light source. Because the parallel light is assumed, r can be thought of as a constant. Let $\alpha_d = L_0 \rho_d / (r^2 \pi)$, $\alpha_s = L_0 \rho_s / r^2$, f is then expanded as:

$$f(\theta_i, \theta_o, \sigma) = \alpha_d \cos \theta_i + \alpha_s \sqrt{\frac{\cos \theta_i}{\cos \theta_o}} \frac{\exp[-\tan^2 \sigma / \beta^2]}{4\pi\beta^2} \quad (4)$$

where the diffuse coefficient ρ_d and the specular coefficient ρ_s are replaced with α_d and α_s respectively, up to a factor $L_0 / (r^2 \pi)$ and L_0 / r^2 . For the specular term in formula (4), let

$$G(\sigma, \beta) = \frac{\exp[-\tan^2 \sigma / \beta^2]}{4\pi\beta^2} \quad (5)$$

$$e(\theta_i, \theta_o) = \sqrt{\frac{\cos \theta_i}{\cos \theta_o}} \quad (6)$$

and approximate $G(\sigma, \beta)$ with the linear combination of several Gaussians in the same form:

$$G(\sigma, \beta) \approx \sum_{j=1} \omega_j G(\sigma, \beta_j) \quad (7)$$

then substitute (6) and (7) into (4), we get

$$f(\theta_i, \theta_o, \sigma) \approx \alpha_d \cos \theta_i + \sum_{j=1} \alpha_s \omega_j e(\theta_i, \theta_o) G(\sigma, \beta_j) \quad (8)$$

From the above equation, we can see the reflectance function with a Ward model is transformed into a linear combination of a diffuse term and several specular terms with varying roughness. Comparing equation (8) and (1), we

can also find that they are equivalent in essence to each other (let $\lambda_{1,p} = \alpha_d$, $f_1(n_p, v, L) = \cos\theta_i$, at the same time let $\lambda_{j+1,p} = \alpha_s \omega_j$, $f_{j+1}(n_p, v, L) = e(\theta_i, \theta_o)G(\sigma, \beta_j)$, $j=1, 2, \dots$). In other words, all materials on target objects have been represented as a linear combination of a diffuse material and several “pure” specular materials.

Multiple specular materials differ only in their roughness values. In practice, we use $\mathbf{B}=\{\beta_j\}=\{0.800, 0.640, 0.512, 0.410, 0.328, 0.262, 0.210, 0.168, 0.134, 0.107, 0.086, 0.069\}$ to cover any possible roughness. The following figure exhibits the appearances of spheres composed of these specular materials illuminated in a specified light direction (these spheres is called Virtual Reference Spheres, VRS):

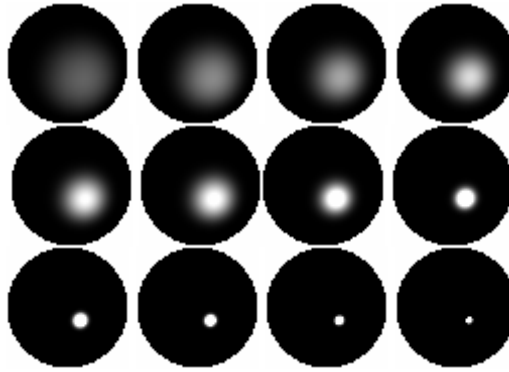


Fig. 2. Twelve rendered specular spheres illuminated in the light direction $[0.4082, 0.4082, -0.8165]^T$. Their roughness correspond the preset roughness collection $\{\beta_j\}$.

The following two figures demonstrate that the Gaussian function $G(\sigma, \beta)$ can be approximated by a collection of other Gaussian functions with various roughness values:

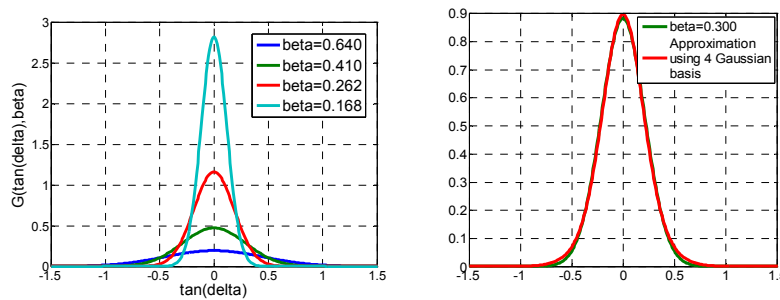


Fig. 3. Left: four Gaussian functions used as basis functions. $\tan(\sigma)$ is used as the independent variable (see formula (5)) Right: the Gaussian function with roughness equal to 0.3000 is approximated by other four Gaussian functions. Their coefficients $\omega_1, \omega_2, \omega_3$ and ω_4 are respectively 0.0003, 0.4843, 0.5768 and 0.0002.

3.1. Recovering the shape and diffuse parameter

After completing the representation for material appearances, estimating the normal per point becomes a search process on all virtual reference spheres. It is detailed as follows:

- (1) Calculate all light directions $\mathbf{L}=\{\mathbf{l}_k\}$ in terms of the specular peak on a shiny steel ball in all test objects images;
- (2) Render the image of the diffuse sphere ($f_1(n,v,l_k)$), and all images of specular spheres ($\{f_j(n,v,l_k), j=2,3,\dots\}$) according to \mathbf{L} . The light intensity L_0 is a preset positive integer (we use 500 in this paper);
- (3) Take a object point p ;
- (4) Search all points on reference spheres for \mathbf{n}_p and $\{\lambda_{j,p}\}$, which minimizes the following objective function:

$$\left\| I_p(L) - \sum_{j=1} \lambda_{j,p} f_j(n_p, v, L) \right\|^2 \quad (9)$$

For color images, equation (9) is actually the quantity accumulated on RGB channel. Also, $\lambda_{j,p}$ is a RGB vector denoting three reflectance coefficients on color channels. The resulting \mathbf{n}_p and $\lambda_{1,p}$ are respectively the accurate normal and the diffuse parameter, while the specular parameters are ambiguous. In implementation, we discarded several smallest pixel values for each point to deal with its potential shading (attached shadow or cast shadow);

- (5) Repeat step (3)-(4), until all object points have been processed;
- (6) Integrate the resulting normal field to construct the triangular mesh.

Executing step (4) is equivalent to solving a overdetermined linear equation system, fulfilled by a matrix pseudo-inverse operation. The resulting \mathbf{n}_p and $\lambda_{1,p}$ are credible, while $\{\lambda_{j,p}, j=2,3,\dots\}$ might be not because for quite a few of points they could not exhibit specular highlights at all under all illumination directions.

3.2. Estimating the specular parameters

In order to estimate specular coefficients reliably, we have made the following assumption (which is not an unreasonable one): points with the same or close diffuse coefficient are thought of as possessing the same material, therefore belonging to a same material category. Thus, estimation of specular parameters for each point evolves to that for each category of material. The diffuse parameter estimated before is naturally chosen as the evidence for clustering materials. In our experiments, the number of categories is pre-defined by observation, then a K-means algorithm is applied to all object points in terms of their diffuse parameter λ_1 .

For each category m , solve its specular coefficients $\{\lambda_j, j=2,3,\dots\}_m$ by minimizing the following objective function while holding the diffuse parameter λ_1 for each point:

$$\sum_{\forall \text{ pixel } p \in \text{class } m} \left\| I_p(L) - \sum_{j=1} \lambda_j f_j(n_p, v, L) \right\|^2 \text{ s.t. } \sum_{j=1} \lambda_j f_j(n_p, v, l_k) \geq 255, \forall I_p(l_k) = 255 \quad (10)$$

The additional constraint in function (10) is used to simulate the saturation effect of a digital camera, i.e. the pixel value will be truncated to a maximum (usually 255) when exposure on that CCD cell location is beyond a physical threshold. The above optimization is actually a linear least square problem with inequation constraints. When implemented, the *lsqlin* function of Matlab is used.

4. Experimental Results

We have tested our algorithm on five real objects, named respectively as Bear, Horse, Rabbit, Heart and Peanut. The light source is a hand-held torch, illuminating these objects from 15-19 directions, and the same number of images was captured by a Canon EOS 5D digital camera. This camera was fixed on a tripod with its optic axis being roughly perpendicular to the base plane of the test objects. The capture was accomplished by an accessory remote-control switch attached to the camera, and the images were uploaded onto a computer connected to the camera via a USB line. The test objects were separated from the background by using edge detection, then were applied the algorithm depicted in section 2. Finally we obtained their surface shapes and reflectance parameters.

The recovering algorithm was written in Matlab code, exporting resultant triangular meshes with reflection parameters for each vertex, which were then imported into a rendering program written in Visual C++ 6.0 and OpenGL 1.2 for display.

Among the five test objects, all but Peanut have specular reflection. From these experimental results, we can see objects shapes are well recovered, and the rendered images are perceptually similar to those original ones, which validate the recovered reflectance parameters (see Fig. 4 and Table 1).

Table 1. The recovering time and relative mean error for five test objects. The relative mean error refers to intensity differences between original and rendered pixels

Object name	Bear	Horse	Rabbit	Heart	Peanut
Recovering time (min.)	45	29	24	17	23
Relative mean error	8.84%	8.02%	4.21%	7.53%	5.29%

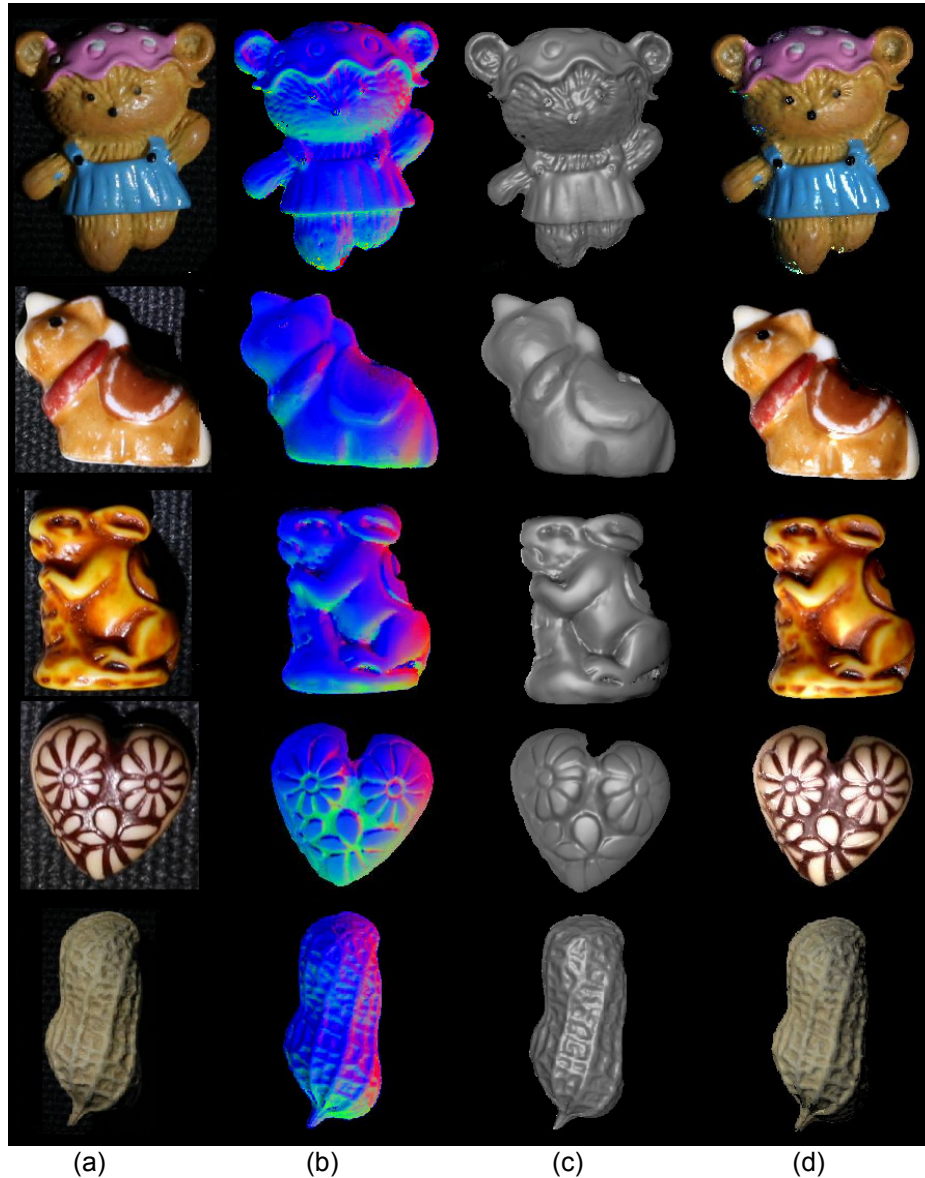


Fig. 4. (a) original test objects images (b) recovered normal maps, the x , y and z component of a normal are respectively encoded in RGB channels (c) reconstructed triangular meshes (d) images rendered according to the recovered shapes and reflection parameters, visually resembling those original ones

We also give rendered images of some objects under novel viewpoints. Because both their shapes and reflectance properties are in hand, the visual appearances under novel viewpoints and light directions can be predicted.



Fig. 5. The left Bear's shape was obtained using the traditional photometric algorithm, while the right shape was obtained using our extended algorithm



Fig. 6. Rendered images for some objects under a novel viewpoint

5. Conclusion

In this paper we proposed an extended photometric stereo algorithm for recover both shape and reflectance properties of a specular object without any removal of specularities. In terms of the recovered shape and reflection parameters, the realistic rendering can be achieved. This algorithm can handle any isotropic reflection, no matter it contains intensively or weakly specular highlight. Slow computation is its main drawback, therefore our future work is to determine the roughness range using a Laplacian-based technique, and further, to reduce the number of basis functions.

6. Acknowledgement

This work was supported by National Basic Research Program of China (973 Program) under Grant No. 2006CB303105, National Natural Science Foundation of China under Grant No. 60873136, Fund for PhD Training under

Grant No. 20050248046, and the Open Project Program of the State Key Lab for Novel Software Technology in Nanjing University. We especially thank Xuezhong Xiao, Na Chu and Yan Wang for their help during the preparation of this paper.

7. References

1. Woodham, R.: Photometric Method for Determining Surface Orientation from Multiple Images. *Optical Engineering*, Vol. 19, No. 1, 139-144. (1980)
2. Keuchi, K.: Determining Surface Orientations of Specular Surfaces by Using the Photometric Stereo Method. *IEEE Transactions on Pattern Analysis and Machine Intelligence*, Vol. 3, No. 6, 661-669. (1981)
3. Nayar, S.K., Ikeuchi, K., Kanade, T.: Determining Shape and Reflectance of Hybrid Surfaces by Photometric Sampling. *IEEE Transactions on Robotics and Automation*, Vol. 6, No. 4, 418-431. (1990)
4. Kay, G., Caelli, T.: Estimating the Parameters of An Illumination Model Using Photometric Stereo. *Graphical Models and Image Processing*, Vol. 57, No. 5, 365-388. (1995)
5. Torrance, K.E., Sparrow, E.M.: Theory for Off-specular Reflection from Roughened Surfaces. *Journal of the Optical Society of America*, Vol. 57, No. 9, 1105-1114. (1967)
6. Georgiades, A.S.: Incorporating the Torrance and Sparrow Model of Reflectance in Uncalibrated Photometric Stereo. In *Proceedings of the 9th International Conference on Computer Vision*. IEEE Computer Society Press, Nice, France, 816-823. (2003)
7. Shen, L., Machida, T., Takemura, H.: Efficient Photometric Stereo Technique for Three-dimensional Surfaces with Unknown BRDF. In *Proceedings of the 5th International Conference on Digital Imaging and Modeling*. IEEE Computer Society Press, Ottawa, Canada, 326-333. (2005)
8. Chung, H.S., Jia, J.: Efficient Photometric Stereo on Glossy Surfaces with Wide Specular Lobes. In *Proceedings of 18th International Conference on Computer Vision and Pattern Recognition*. IEEE Computer Society Press, Santa Barbara, US, 1-8. (1998)
9. Ward, G.: Measuring and Modeling Anisotropic Reflection. In *Proceedings of 21st Annual Conference on Computer Graphics and Interactive Techniques*. Addison-Wesley, Orlando, US, 239-246. (1994)
10. Hertzmann, A., Seitz, S.M.: Example-based Photometric Stereo: Shape Reconstruction with General, Varying BRDFs. *IEEE Transactions on Pattern Analysis and Machine Intelligence*, Vol. 27, No. 8, 1254-1264. (2005)
11. Alldrin, N., Zickler, T., Kriegman, D.: Photometric Stereo with Non-parametric and Spatially-varying Reflectance. In *Proceedings of 28th International Conference on Computer Vision and Pattern Recognition*. IEEE Computer Society Press, Anchorage, US, 1-8. (2008)
12. Chen, T.B., Goesele, M., Seidel, H.P.: Mesostructure from Specularity. In *Proceedings of 26th International Conference on Computer Vision and Pattern Recognition*. IEEE Computer Society Press, New York, US, 825-832. (2006)
13. Francken, Y., Cuypers, T., Mertens, T., Gielis, J., Bekaert, P.: High Quality Mesostructure Acquisition Using Specularities. In *Proceedings of 28th International Conference on Computer Vision and Pattern Recognition*. IEEE Computer Society Press, Anchorage, US, 1-7. (2008).

Zuoyong Zheng, Lizhuang Ma, Zhong Li, and Zhihua Chen

Zuoyong Zheng is currently a PhD student at the Department of Computer Science, Shanghai Jiaotong University, China. He has participated in several open projects supported by national level scientific research funds. His research interests include shape modeling and realistic rendering

Lizhuang Ma is a professor of the Department of Computer Science, Shanghai Jiaotong University, China. His research areas are computer graphics and computer aided geometry design. He has (co-)authored around 160 research papers, and has been the chair and/or member of program committees of many international conferences.

Zhong Li is an associate professor of mathematics and science at Zhejiang Sci-Tech University. He received the Ph.D. degree in mathematics from Zhejiang University in 2003. He was a post-doctoral fellow of computer science at Shanghai Jiao Tong University from 2004 to 2006 and was a visiting scholar of computer science division at University of California at Berkeley, U.S.A. from 2007 to 2008. His current research interests are mesh processing and garment CAD.

Zhihua Chen is a lecturer in the School of Information and Engineering at East China University of Science and Technology. So far, he has authored over 20 research papers. He is a member of CCF(China Computer Federation). His research interests include CG, CAD and Compute Animation.

Received: May 02, 2009; Accepted: July 12, 2009.